

Dynamical mean field study of the two-dimensional disordered Hubbard model

Yun Song,^{1,2} R. Wortis,¹ and W. A. Atkinson¹¹*Department of Physics and Astronomy, Trent University, 1600 West Bank Drive, Peterborough, Ontario, Canada K9J 7B8*²*Department of Physics, Beijing Normal University, Beijing 100875, China*

(Received 23 January 2008; published 21 February 2008)

We study the paramagnetic Anderson-Hubbard model using an extension of dynamical mean field theory (DMFT), known as statistical DMFT, that allows us to treat disorder and strong electronic correlations on equal footing. An approximate nonlocal Green's function is found for individual disorder realizations and then configuration averaged. We apply this method to two-dimensional lattices with up to 1000 sites in the strong disorder limit, where an atomic-limit approximation is made for the self-energy. We investigate the scaling of the inverse participation ratio at quarter- and half-filling, and find a nonmonotonic dependence of the localization length on the interaction strength. For strong disorder, we do not find evidence for an insulator-metal transition, and the disorder potential becomes unscreened near the Mott transition. Furthermore, strong correlations suppress the Altshuler-Aronov density of states anomaly near half-filling.

DOI: [10.1103/PhysRevB.77.054202](https://doi.org/10.1103/PhysRevB.77.054202)

PACS number(s): 71.10.Fd, 71.27.+a, 71.30.+h, 73.20.Fz

I. INTRODUCTION

The physical properties of interacting disordered materials are often qualitatively different from their noninteracting counterparts. For example, it has long been known that noninteracting quasiparticles in two-dimensional (2D) materials are localized by arbitrarily weak disorder; however, there is evidence that interactions can drive an insulator-metal transition in 2D.¹ Similarly, there is a growing awareness that disorder can fundamentally alter the physical properties of interacting systems. This arises in a number of transition-metal oxides,²⁻⁵ where the predominantly *d*-orbital character of the conduction electrons results in a large intraorbital (on-site) Coulomb interaction relative to the bandwidth. These materials are of interest because they have an interaction-driven insulating (Mott-insulating) phase and because of the variety of exotic phases, such as high temperature superconductivity, which appear near half-filling. However, transition-metal oxides are typically doped by chemical substitution and, with few exceptions, are intrinsically disordered. At present, there is little consensus on the effects of this disorder, particularly near the transition to the Mott-insulating phase.

Here, we discuss the effects of strong electronic correlations on disordered 2D materials via a numerical study of the Anderson-Hubbard model,

$$\hat{H} = -t \sum_{\langle i,j \rangle} \sum_{\sigma} c_{i\sigma}^{\dagger} c_{j\sigma} + \sum_i (U \hat{n}_{i\uparrow} \hat{n}_{i\downarrow} + \epsilon_i \hat{n}_i), \quad (1)$$

where $\langle i,j \rangle$ refers to nearest-neighbor lattice sites i and j ; $\sigma = \uparrow, \downarrow$ is the spin index; and $\hat{n}_i = \hat{n}_{i\uparrow} + \hat{n}_{i\downarrow}$, where $\hat{n}_{i\sigma} = c_{i\sigma}^{\dagger} c_{i\sigma}$ is the local charge-density operator. The model has four parameters: the kinetic energy t , the intraorbital Coulomb interaction U , the width W of the disorder-potential distribution, and the chemical potential μ . Disorder is introduced through randomly chosen site energies ϵ_i , which in this work are box distributed according to $P(\epsilon_i) = W^{-1} \Theta(W/2 - |\epsilon_i|)$.

For $U=0$, it is well understood that the single-particle eigenstates of Eq. (1) are Anderson localized for $W > W_c$, where W_c is the critical disorder and $W_c=0$ in two and fewer

dimensions. For $W=0$, and at half-filling (i.e., $n=1$, where n is the charge density), there is a critical interaction strength U_c such that the model is a gapped Mott insulator for $U > U_c$ and (neglecting possible broken-symmetry phases) a strongly correlated metal for $U < U_c$ or for $n \neq 1$. There is evidence that the Mott transition is fundamentally different in the presence of disorder. For example, some work have shown that $U_c=0$ in clean low-dimensional systems with nested Fermi surfaces,⁶⁻⁹ while in the disordered case, U_c is not only nonzero, but rapidly becomes of the order of the bandwidth as a function of W .⁹⁻¹¹ In fact, it has become clear through numerous studies that the general U - W - n phase diagram is complicated and also potentially contains superconducting, antiferromagnetic, and spin glass phases.¹¹⁻¹⁴ Much of the recent progress has been for infinite-dimensional systems,¹⁴⁻²¹ and the applicability of this work to two and three dimensions is not well established. A recent focus has been the extent to which interactions screen the disorder potential^{19,21-23} and whether screening may lead to an insulator-metal transition.^{12,22-24} In particular, some calculations show perfect screening near the Mott transition.^{19,21}

Part of the confusion surrounding the Anderson-Hubbard phase diagram stems from the variety of theoretical approaches that have been applied. Self-consistent Hartree-Fock (HF) calculations¹¹⁻¹³ treat the disorder potential exactly, but do not capture the strong-correlation physics of the Mott transition. Dynamical mean field theory (DMFT) approaches contain the necessary strong-correlation physics, but are based on a local approximation that generally precludes exact treatment of disorder. A variety of coherent potential approximation (CPA) and CPA-like approximations have been employed in conjunction with DMFT.¹⁴⁻²⁰ While the CPA reproduces some disorder-averaged quantities accurately, e.g., the density of states (DOS) in the noninteracting limit, it fails to reproduce quantities that depend on explicit knowledge of spatial correlations between lattice sites. As a notable example, the CPA fails to predict the Altshuler-Aronov DOS anomaly which appears at the Fermi energy in disordered metals.²⁵ Quantum Monte Carlo^{22,23} and exact diagonalization²⁴ (ED) methods treat both disorder and interactions exactly, but suffer from severe finite-size limitations,

typically generate only equal-time correlations, and (in the case of quantum Monte Carlo) suffer from the fermion sign problem.

In this work, we use an extension of DMFT, known as statistical DMFT,²⁶ that incorporates both strong correlations and an exact treatment of the disorder potential. By varying U for a fixed disorder strength, we are able to move smoothly from the well-understood weakly correlated regime into the unknown territory of strongly correlated disordered systems. Because our approach retains spatial correlations between the local self-energy at different lattice sites, but can also be applied to reasonably large lattices in finite dimensions, it provides a bridge between the various methods described above. Up to now, statistical DMFT has been applied only on a Bethe lattice. Here, we work with a two-dimensional square lattice and present results for the density of states, scaling of the inverse participation ratio, and the screened potential.

II. METHOD

We focus on paramagnetic solutions on the 2D square lattice, for which the noninteracting bandwidth is $D=8t$. On an N -site lattice, the single-particle Green's function can be expressed as an $N \times N$ matrix in the site index:

$$\mathbf{G}(\omega) = [\omega \mathbf{I} - \mathbf{t} - \boldsymbol{\epsilon} - \boldsymbol{\Sigma}(\omega)]^{-1}, \quad (2)$$

with \mathbf{I} the identity matrix, \mathbf{t} the matrix of hopping amplitudes, $\boldsymbol{\epsilon}$ the diagonal matrix of site energies ϵ_i , and $\boldsymbol{\Sigma}(\omega)$ the matrix of self-energies. The matrix \mathbf{t} has nonzero matrix elements $t_{ij} = -t$ for i and j corresponding to nearest-neighbor sites. We assume that $\boldsymbol{\Sigma}(\omega)$ is local, having only diagonal matrix elements $\Sigma_i(\omega)$.

The iteration cycle begins with the calculation of $\mathbf{G}(\omega)$ from Eq. (2). For each site i , one defines a Weiss mean field $\mathcal{G}_i^0(\omega) = [G_{ii}(\omega)^{-1} + \Sigma_i(\omega)]^{-1}$, where $G_{ij}(\omega)$ are the matrix elements of $\mathbf{G}(\omega)$. As in the conventional DMFT, one then solves for the full Green's function $\mathcal{G}_i(\omega)$ of an Anderson impurity whose noninteracting Green's function is $\mathcal{G}_i^0(\omega)$. The self-energy is then updated according to $\Sigma_i^{new}(\omega) = \mathcal{G}_i^0(\omega)^{-1} - \mathcal{G}_i(\omega)^{-1}$, and the iteration cycle is restarted. In the disorder-free case, this algorithm reduces to the conventional DMFT.

We have used the Hubbard-I (HI) approximation as a solver for $\mathcal{G}_i(\omega)$, for which, in the paramagnetic case, $\mathcal{G}_i(\omega) = [\mathcal{G}_i^0(\omega)^{-1} - \Sigma_i^{HI}(\omega)]^{-1}$, where

$$\Sigma_i^{HI}(\omega) = U \frac{n_i}{2} + \frac{U^2 \frac{n_i}{2} \left(1 - \frac{n_i}{2}\right)}{\omega - \epsilon_i - U \left(1 - \frac{n_i}{2}\right)}, \quad (3)$$

and $n_i \equiv \langle \hat{n}_i \rangle$ is self-consistently determined for each site. The HI approximation is the simplest improvement over HF that generates both upper and lower Hubbard bands. When either the HF or HI approximations are used as a solver, the DMFT result is, in fact, equivalent to the result obtained directly from the corresponding approximation. However, the

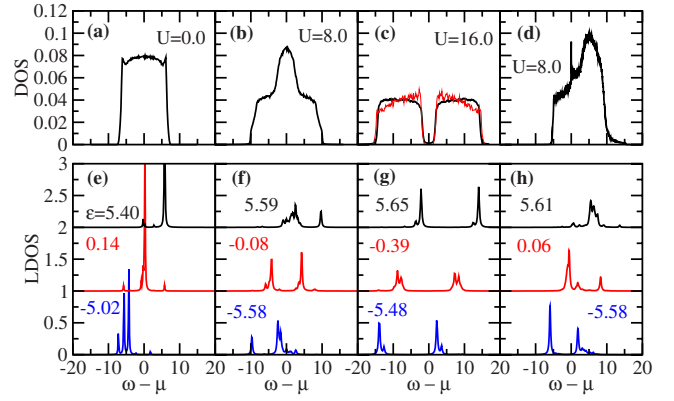


FIG. 1. (Color online) Density of states. (a)–(c) Total DOS for $W=12t$, $n=1$, and different U . Results have been averaged over 1000 samples and are for an $N=20 \times 20$ site square lattice. ED results, averaged over 10000 samples, for a four-site lattice (red) are also shown in (c). (d) DOS for $n=0.5$. Also shown (e)–(g) is the LDOS for three arbitrarily chosen sites (site energies indicated in the figure). (e) is for the same parameters as (a), (f) as (b), etc. Energies are in units of t .

statistical-DMFT procedure outlined above, applied to a physical lattice, and hence implemented through a matrix inversion [Eq. (2)], is very computationally intensive. In particular, it can be difficult to achieve a converged self-consistent solution to the N coupled equations for $\Sigma_i(\omega)$. This work, aside from being a simple improvement beyond HF, represents an important proof of principle regarding the feasibility of this statistical DMFT approach.

The fact that we are studying disordered systems bears on two important and related issues: (i) the accuracy of the HI approximation and (ii) the validity of single-site (as opposed to cluster or cellular) DMFT in a finite-dimensional system. The strengths and weaknesses of the HI approximation are well documented in the clean limit: it is exact in the atomic limit ($U/t \gg 1$), but is nonconserving and fails to satisfy Luttinger's theorem.²⁷ However, it is uniquely effective in low-dimensional disordered systems because $W/t \gg 1$ corresponds to the atomic limit for arbitrary U in systems with finite coordination number. This is in apparent contradiction to the general result that DMFT is only exact in infinite dimensions, while nonlocal terms in the self-energy, neglected in DMFT, can have a dramatic effect on the Mott transition in 2D.^{28,29} In the disordered case, however, we have compared our results with ED studies on small clusters³⁰ and have found qualitative agreement for $W=12t$ (i.e., $W=1.5D$), which is the focus of the current work. By pushing the system toward the atomic limit, strong disorder both enhances the accuracy of the HI approximation and also reduces the importance of nonlocal terms in the self-energy.

III. RESULTS

The local density of states (LDOS) is extracted from the Green's function as $\rho(\mathbf{r}_i, \omega) = -\pi^{-1} \text{Im} G_{ii}(\omega)$ and the DOS is $\rho(\omega) = N^{-1} \sum_i \rho(\mathbf{r}_i, \omega)$. Figures 1(a)–1(c) show the evolution of the DOS as a function of U for fixed W at half-filling. There

is a transition from a single band to a gapped Mott-insulating state at a critical interaction $U_c \approx 12.5t$. In contrast, the LDOS [Figs. 1(e)–1(g)] develops a local Mott gap at much smaller values of U . We note that, at most sites, the noninteracting LDOS has a single strong resonance near the bare site energy [Fig. 1(e)], indicating proximity to the atomic limit where HI becomes exact. The coordination number of the lattice determines the disorder strength required to approach the atomic limit. In lattices with infinite coordination number, each site couples to a continuum of states and the atomic limit is never reached for finite W . Thus, somewhat paradoxically, DMFT with the HI solver works best, in disordered systems, for lattices with low coordination number.

It is useful to compare the DOS evolution in Fig. 1 with existing published work. First, we note that the Mott transition occurs at $U_c \approx W$ in both our DMFT and ED calculations. This is consistent with quantum Monte Carlo results for three dimensions,⁹ as well as infinite-dimensional DMFT results,¹⁵ but U_c is somewhat larger than found in one dimension.¹⁰ Our U_c is also significantly larger than in unrestricted HF calculations for three dimensions;¹¹ however, in HF calculations, the metal-insulator transition is of the Slater type and could, therefore, be expected to respond differently to disorder.

Previously published results for the DOS near the Mott transition in the large-disorder limit, to our knowledge, are for infinite dimensions where CPA-like approximations can be made. The main distinction between our results and those for infinite dimensions is the quasiparticle resonance due to Kondo screening of the local moments that appears at the Fermi energy for $U \sim U_c$ in the latter case.^{15,18–20} (The peak at $\omega = \mu$ for $U = 8t$ comes from the overlap of the lower and upper Hubbard bands.) The HI solver cannot give such a peak; however, ED calculations for small clusters³⁰ also find no resonance at any U . In particular, Fig. 1(c) shows ED results for parameters corresponding to a maximum quasiparticle resonance height in Refs. 15 and 20. The difference between our results and those for infinite dimensions might seem unsurprising since there is also no resonance in the clean limit in two dimensions.²⁹ However, the reason for this absence appears to be different in the clean and disordered systems. The lack of a quasiparticle resonance in clean 2D systems has been attributed to nonlocal terms in the self-energy,²⁹ terms which are not included in HI. These nonlocal terms describe short-ranged antiferromagnetic correlations whose effect is to suppress U_c to zero in the clean limit.^{7,8,28} In our work, the absence of a quasiparticle peak stems from the calculations being in the atomic limit. That the same physics controls the ED results is supported by the fact that U_c is nearly identical in HI and ED calculations. It, therefore, appears as if the limitations of the HI solver do not hide key physics in the large-disorder limit.

The DOS at quarter-filling Fig. 1(d) *does* have a peak at the Fermi energy, but the origin of this peak is unrelated to strong correlations. Paramagnetic HF calculations²⁵ have shown that nonlocal charge-density correlations lead to a positive DOS anomaly at the Fermi level in disordered metals when the interaction is zero range and repulsive. This Altshuler-Aronov DOS anomaly is absent at half-filling in our calculations, in contradiction with the HF calculations,

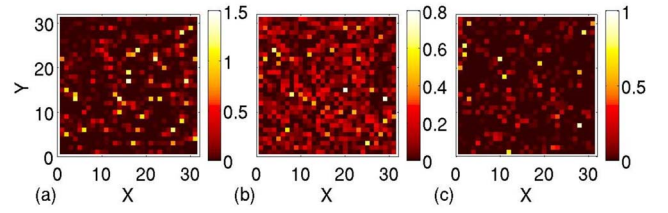


FIG. 2. (Color online) Local density of states for a single disorder realization at $\omega = \mu$ and $W = 12t$, for (a) $U = 0$, (b) $U = 8t$, and (c) $U = 12t$ for an $N = 32 \times 32$ site lattice and $n = 1$.

indicating that strong correlations suppress the peak. We will discuss this point below.

In Fig. 2, $\rho(\mathbf{r}, \mu)$ is plotted for different values of U for a particular disorder configuration. At $U = 0$, sites which have significant spectral weight at $\omega = \mu$ are typically isolated from one another, consistent with electrons being Anderson-localized. The LDOS is more homogeneous for $U = 8t$ than for $U = 0$, consistent with an interaction-driven delocalizing effect. However, at $U = 12t$, the LDOS is again highly inhomogeneous.

The inverse participation ratio (IPR)

$$I_2(\omega, N) = \frac{\sum_{i=1}^N \rho(\mathbf{r}_i, \omega)^2}{\left[\sum_{i=1}^N \rho(\mathbf{r}_i, \omega) \right]^2} \quad (4)$$

provides a quantitative measure of the inhomogeneity of $\rho(\mathbf{r}, \omega)$. The IPR can also be used to distinguish extended and localized states since $\lim_{N \rightarrow \infty} I_2(\omega, N) = 0$ for the former and is nonzero for the latter. It is important to note that the frequency ω used in the calculation of $\mathbf{G}(\omega)$ in Eq. (2) contains, by necessity, a small imaginary component $i\gamma$. Scaling quantities such as the IPR that are derived from $\mathbf{G}(\omega)$ generally depend on γ .³¹ In our scaling calculations, we have taken $\gamma \propto 1/N$ such that the ratio of γ to the level spacing remains constant. As shown in Fig. 3(a) for the noninteracting case, the effect of γ is to reduce $I_2(\omega, N)$, such that our results represent a lower bound on the true ($\gamma = 0$) IPR. The IPR scaling at half-filling is shown in Fig. 3(b) for $\omega = \mu$. For each value of U , we extrapolate a limiting value $I_2(\mu, \infty)$. We then define a localization length $\xi = I_2(\mu, \infty)^{-1/d}$, where d is the dimension of the system.³² For finite γ , $I_2(\mu, \infty)^{-1/d}$ gives an upper bound for ξ .

Figures 3(c) and 3(d) illustrate the effect of strong correlations on localization. While the HI results agree closely with self-consistent HF calculations for small U , the discrepancy between the methods grows as U is increased. In the weakly correlated small- U regime, ξ grows with U , consistent with increased screening of the impurity potential.^{19,23} For large U , however, ξ is a *decreasing* function of U and is smaller near the Mott transition than in the $U = 0$ case. As we discuss below, this can be partially attributed to a decrease in screening due to strong correlations, although screening no

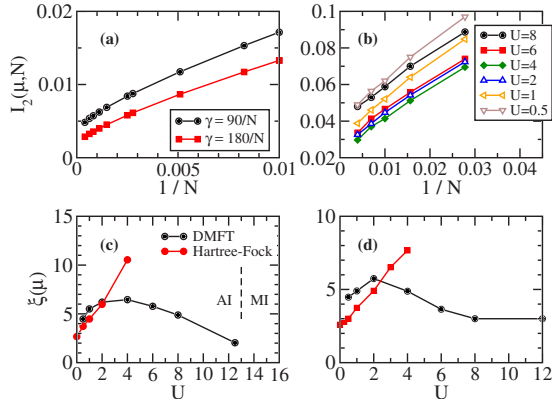


FIG. 3. (Color online) IPR scaling with system size for $W=12t$. Shown are (a) the dependence of the IPR on γ for $U=0$, (b) the scaling of the IPR with $\gamma=4t/N$ and $n=1$, and the dependence of the localization length (defined in text) on U at (c) $n=1$ and (d) $n=0.5$. All curves are for $\omega=\mu$. Anderson-insulating (AI) and Mott-insulating (MI) phases are indicated in (c).

longer provides a complete framework for understanding the evolution of ξ .

To understand better the localizing effect of strong correlations, we define a screened potential^{19,20,23} V_i based on the HF site energy: $V_i = \epsilon_i + U \frac{n_i - n}{2}$.²³ Plots of both n_i and V_i as a function of ϵ_i are shown in Fig. 4. In the weakly correlated limit ($U=t$), n_i is approximately linear in ϵ_i over a wide range and $V_i \approx \epsilon_i(1 - U\chi_{ii})$ with $\chi_{ii} = -dn_i/d\epsilon_i$. Since χ_{ii} depends only weakly on U , V_i is a decreasing function of U . In the strongly correlated limit ($U=8t$), n_i is a nonlinear function of ϵ_i . For $|\epsilon_i| < U/2$, $n_i \approx 1$ and $\chi_{ii} = 0$, such that these sites are unscreened (i.e., $V_i = \epsilon_i$). There are, therefore, two limits in which screening is small at half-filling: $U \ll W$, where the interaction is too weak to screen the impurity potential, and $U \sim W$, where strong correlations enforce single occupancy of most sites. We note that the absence of an Altshuler-Aronov DOS anomaly near half-filling can be understood in this context: strong correlations suppress the local response of the charge density to the impurity potential.

A measure of the screening is given by the relative variance ΔV^2 , defined as the variance of V_i divided by the vari-

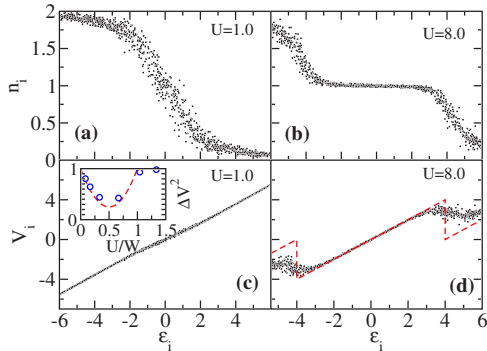


FIG. 4. (Color online) [(a) and (b)] Local charge density and [(c) and (d)] corresponding screened potential as a function of site energy. The screened potential in the $t=0$ limit (red dashed) is also shown in (d). The relative variance of V_i (circles) is shown (inset) along with the $t=0$ result (dashed curve).

ance of ϵ_i . Our numerical results (Fig. 4) show that ΔV^2 is a nonmonotonic function of U , obtaining a minimum at $U \approx W/2$ and approaching $\Delta V^2=1$ for $U \rightarrow 0$ and $U \geq W$. At a qualitative level, this is consistent with the nonmonotonic dependence of ξ on U , since one expects ξ to be large when ΔV^2 is small. There are, however, quantitative discrepancies which show that ΔV^2 does not tell the whole story. First, ξ does not obtain its maximum at $U=W/2$, where ΔV^2 obtains its minimum. Second, ξ is smaller at large U than at $U=0$, indicating that states near the Mott transition are more strongly localized than at $U=0$.

Our results for the IPR are consistent with recent quantum Monte Carlo calculations of the dc conductivity^{24,23} which find a similar nonmonotonic dependence on U . The results for the screened potential, however, are inconsistent with infinite-dimensional DMFT results.^{19,20} In Ref. 19, impurities are found to be perfectly screened (i.e., $\Delta V^2 \rightarrow 0$) at the Mott transition, which would correspond to a divergent ξ in our calculations. Near the Mott transition, Ref. 21 found that sites with $|\epsilon_i| < U/2$ are perfectly screened. Both of these results are opposite to what we have found here.

There are two important distinctions between our calculation and those of Refs. 19 and 21, both of which contribute to these opposing results on screening. First, Refs. 19 and 21 use an effective medium approach for the disorder potential that results in metallic behavior for small U . This is reasonable in high dimensions where Anderson localization only occurs for strong disorder. Our exact treatment of the disorder potential, on the other hand, allows us to describe the Anderson localized phase that occurs in two dimensions for small U . Whereas the LDOS is continuous and relatively uniform in the metallic case, it is inhomogeneous and dominated by small numbers of resonances in the Anderson insulating phase [cf. Fig. 1(f)]. The local charge susceptibility χ_{ii} is suppressed for sites with small LDOS at the Fermi level, and screening in the Anderson-insulating phase is consequently expected to be less than in the metallic phase. The second distinction is the quasiparticle resonance which arises in the infinite-dimensional case but does not occur in our calculations. This resonance is a key factor in the perfect screening found in Refs. 19 and 21.

In conclusion, we have studied the 2D Anderson-Hubbard model at half- and quarter-filling, in the limit of large disorder using statistical DMFT. We have calculated the localization length ξ from the inverse participation ratio, and find that it varies nonmonotonically with the strength of the interaction: at small U , the interaction screens the impurity potential, but at large U , strong correlations reduce the screening. As a consequence, the Altshuler-Aronov DOS anomaly is suppressed at half-filling. For strong disorder, we find no evidence for an insulator-metal transition nor for enhanced screening near the Mott transition.

ACKNOWLEDGMENTS

We thank R. J. Gooding and E. Miranda for helpful conversations. We acknowledge Trent University, NSERC of Canada, CFI, and OIT for financial support. Some calculations were performed using the High Performance Computing Virtual Laboratory (HPCVL).

- ¹S. V. Kravchenko and M. P. Sarachik, Rep. Prog. Phys. **67**, 1 (2004).
- ²D. D. Sarma *et al.*, Phys. Rev. Lett. **80**, 4004 (1998).
- ³S. Nakatsuji, V. Dobrosavljević, D. Tanasković, M. Minakata, H. Fukazawa, and Y. Maeno, Phys. Rev. Lett. **93**, 146401 (2004).
- ⁴K. W. Kim, J. S. Lee, T. W. Noh, S. R. Lee, and K. Char, Phys. Rev. B **71**, 125104 (2005).
- ⁵J. Kim, J. Y. Kim, B. G. Park, and S. J. Oh, Phys. Rev. B **73**, 235109 (2006).
- ⁶Elliott H. Lieb and F. Y. Wu, Phys. Rev. Lett. **20**, 1445 (1968).
- ⁷J. E. Hirsch, Phys. Rev. B **31**, 4403 (1985).
- ⁸S. R. White, D. J. Scalapino, R. L. Sugar, E. Y. Loh, J. E. Gubernatis, and R. T. Scalettar, Phys. Rev. B **40**, 506 (1989).
- ⁹Y. Otsuka and Y. Hatsugai, J. Phys.: Condens. Matter **12**, 9317 (2000).
- ¹⁰Y. Otsuka, Y. Morita, and Y. Hatsugai, Phys. Rev. B **58**, 15314 (1998).
- ¹¹M. A. Tusch and D. E. Logan, Phys. Rev. B **48**, 14843 (1993).
- ¹²D. Heidarian and N. Trivedi, Phys. Rev. Lett. **93**, 126401 (2004).
- ¹³F. Fazileh, R. J. Gooding, W. A. Atkinson, and D. C. Johnston, Phys. Rev. Lett. **96**, 046410 (2006).
- ¹⁴M. Ulmke, V. Janiš, and D. Vollhardt, Phys. Rev. B **51**, 10411 (1995).
- ¹⁵K. Byczuk, W. Hofstetter, and D. Vollhardt, Phys. Rev. Lett. **94**, 056404 (2005).
- ¹⁶M. Balzer and M. Potthoff, Physica B **359-361**, 768 (2005).
- ¹⁷M. S. Laad, L. Craco, and E. Müller-Hartmann, Phys. Rev. B **64**, 195114 (2001).
- ¹⁸P. Lombardo, R. Hayn, and G. I. Japaridze, Phys. Rev. B **74**, 085116 (2006).
- ¹⁹D. Tanasković, V. Dobrosavljević, E. Abrahams, and G. Kotliar, Phys. Rev. Lett. **91**, 066603 (2003).
- ²⁰M. C. O. Aguiar, V. Dobrosavljević, E. Abrahams, and G. Kotliar, Phys. Rev. B **73**, 115117 (2006);
- ²¹M. C. O. Aguiar, V. Dobrosavljević, E. Abrahams, and G. Kotliar, arXiv:0704.0450v1 (unpublished).
- ²²B. Srinivasan, G. Benenti, and D. L. Shepelyansky, Phys. Rev. B **67**, 205112 (2003).
- ²³P. B. Chakraborty, P. J. H. Denteneer, and R. T. Scalettar, Phys. Rev. B **75**, 125117 (2007).
- ²⁴R. Kotlyar and S. Das Sarma, Phys. Rev. Lett. **86**, 2388 (2001).
- ²⁵B. L. Altshuler and A. G. Aronov, *Electron-Electron Interactions in Disordered Systems*, Modern Problems in Condensed Matter Sciences Vol. 10 (North-Holland, Amsterdam, 1985).
- ²⁶V. Dobrosavljević and G. Kotliar, Phys. Rev. Lett. **78**, 3943 (1997); Philos. Trans. R. Soc. London, Ser. A **356**, 57 (1998); E. Miranda and V. Dobrosavljević, Rep. Prog. Phys. **68**, 2337 (2005).
- ²⁷F. Gebhard, *The Mott Metal-Insulator Transition: Models and Methods*, Springer Tracts in Modern Physics Vol. 137 (Springer, New York, 1997).
- ²⁸S. Moukouri and M. Jarrell, Phys. Rev. Lett. **87**, 167010 (2001).
- ²⁹Y. Z. Zhang and Masatoshi Imada, Phys. Rev. B **76**, 045108 (2007).
- ³⁰S. Bulut and W. A. Atkinson (unpublished).
- ³¹Y. Song, W. A. Atkinson, and R. Wortis, Phys. Rev. B **76**, 045105 (2007); R. Wortis, Yun Song, and W. A. Atkinson, arXiv:0709.0713 (unpublished).
- ³²Y. V. Fyodorov and A. D. Mirlin, Phys. Rev. Lett. **69**, 1093 (1992).